Available online at www.sciencedirect.com

SciVerse ScienceDirect

journal homepage: www.elsevier.com/locate/jmbbm

Research paper

Lubrication of metal-on-metal hip joints: The effect of protein content and load on film formation and wear

C. Myant, R. Underwood, J. Fan, P.M. Cann*

Tribology Group, Department of Mechanical Engineering, Imperial College London, United Kingdom

ARTICLE INFO

Article history:
Received 24 June 2011
Received in revised form
12 September 2011
Accepted 14 September 2011
Published online 22 September 2011

Keywords:
Artificial hip joint
Bovine calf serum
Albumin
Globulin
Film thickness
Wear
CoCrMo alloy

ABSTRACT

Lubricant films were measured for a series of bovine serum and protein containing (albumin, globulin) saline solutions for CoCrMo femoral component sliding against a glass disc. Central film thickness was measured by optical interferometry as a function of time (constant mean speed: 0 and 10 mm/s) and variable mean speed (0–50 mm/s). The effect of load (5–20 N) on film thickness was also studied. The development of the wear scar on the CoCrMo surface was monitored by measuring the width of the contact zone during the film thickness tests. The results showed film thickness increased with time for both the static and sliding tests. Films formed in the static, loaded test were typically in the range of 3–40 nm. The globulin containing solutions formed the thickest films. In the sliding tests a wear scar rapidly formed on the implant component for the bovine serum and albumin fluids, negligible wear was observed for the globulin solutions. Film thickness increased with sliding time for all test solutions and was much greater than predicted by isoviscous EHL models. The film increase was found to correlate with increasing wear scar size and thus decreasing contact pressure. A new lubricating mechanism is proposed whereby during sliding the fluid undergoes bulk phase separation rheology, so that an elevated protein phase forms in the inlet zone. This protein phase is a high-viscosity biphasic matrix, which is periodically entrained into the contact forming a thick protective hydro-gel film. One of the main findings of this study is that film thickness was very sensitive to load; to a much greater extent than predicted by EHL models. Thus film formation in MoM hip joints is very susceptible to high contact pressures which might be due to implant misalignment and edge-loading.

1. Introduction: artificial joint lubrication

Artificial joint procedures and in particular the replacement of hips and knees continue to become more frequent. Recently the UK National Joint Registry (2010) reported a total of 71,021 primary hip and 8309 revision procedures for 2008/2010 in England alone. In addition there is increasing usage of larger femoral heads; in 2009 47% of hips had a head size of 32 mm or greater compared to 21% in 2006 and 6% in 2003 which is due in part to the greater use of LHMoM resurfacings (NJR 2010). However, concern over postoperative lesions (Revell et al., 1997) has prompted a re-evaluation of the performance of LHMoMs which culminated in the issue of a Medical Device Alert by the *Medicines and*

* *Corresponding author.* Tel.: +44 2075947236.
E-mail address: connor.myant@imperial.ac.uk (C. Myant).

1751-6161/$ - see front matter © 2011 Elsevier Ltd. All rights reserved.
doi:10.1016/j.jmbbm.2011.09.008

Abbreviations

BCS	Bovine calf serum
CoCrMo	FS75 Cobalt–chromium–molybdenum alloy
CW_{start} CW_{end}	Effective contact width measured at the start and end of the test
CW_r	Relative effective contact width CW_{end}/CW_{start}
EHL	Elastohydrodynamic lubrication
LHMoM	Large head metal-on-metal
MoM	Metal-on-metal
SF	Synovial fluid
THR	Total hip replacement
UHMWPE	Ultra high molecular weight polyethylene

Healthcare products Regulatory Agency (MHRA, 2010) and the withdrawal of some brands from the market. The NJR (2010) reported overall revision rates of "2.9% *of the patients had a revision of their hip replacement within five years. The lowest revision rates were seen in patients who received a cemented prosthesis (five year revision rate of* 2.0%) *and the highest in those who had a LHMoM THR (five year revision rate of* 7.8%)". There are a number of underlying factors which contribute to high LHMoM failure, which include; design, surgeon and patient issues. The most usual explanation is that LHMoM hips are susceptible to non-optimum positioning particularly the inclination angle of the acetabular cup. High inclination angles are thought to contribute to edge-loading which is associated with high wear rates (Langton et al., 2008). The results from hip simulator tests (Smith et al., 2011) and fluid film modelling (Dowson, 2006) predict that the larger head size should significantly improve performance and implant life. However the revision rates belie this prediction and one possible explanation for this disparity is that the fundamental lubrication mechanisms are different and that patient synovial fluid chemistry plays a role.

Wear of artificial joints is controlled by the properties of the implant material and lubricating film. The effects of non-optimum implant position, patient gait, implant design and synovial fluid chemistry will be reflected in the lubricant film properties. The relevant properties include film thickness during articulation and chemical composition. Lubricating film formation over the gait cycle is usually ascribed to hydrodynamic mechanisms due to the effects of fluid entrainment and squeeze film (Dowson, 2006). The lubricant is modelled as a simple continuum fluid with a Newtonian rheology (Cooke et al., 1978; Dowson, 2006). An alternative mechanism is boundary lubrication due to surface films formed by phospholipids or proteins contained in the periprosthetic synovial fluid (Bell et al., 2001; Widmer et al., 2001).

In an earlier paper (Fan et al., 2011) we reported a new mechanism for film formation with protein containing solutions. The research showed model synovial fluid solutions formed much thicker films than expected which was attributed to protein-agglomeration close to the contact. This formed a reservoir of high-viscosity material in the inlet region which passed through the contact developing a relatively thick lubricant film. Post-test examination of the femoral head revealed the formation of gelatinous deposits close to the wear scar in the inlet region (Fan et al., 2011). There are a number of papers in the research literature reporting the formation of organic deposits on implant surfaces (Wimmer et al., 2003). The concentration and type of proteins in SF affect implant wear (Sawae et al., 2008; Wang et al., 2003) although the relationship is not clear and there is very little reported work for MoM implants. There are significant differences between healthy and periprosthetic SF (Delecrin et al., 1994; Kitano et al., 2001) and this might be a further factor determining premature joint failure.

Kitano et al. (2001) describe healthy and periprosthetic SF as containing a mixture of large and surface active molecules including proteins (albumin and γ-globulin), phospholids, hyaluronan. Kitano et al. (2001) go on to list the total protein content of healthy SF in the range 18–20 mg/ml, which increases in periprosthetic and diseased SF to 30–50 mg/ml. The most abundant protein is given as albumin, which is typically found with a concentration range of 20–39 mg/ml in periprosthetic SF and 7–18 mg/ml in healthy. The concentration of globulin also increases from 0.5–2.9 mg/ml in healthy and from 4.6–15.4 mg/ml in periprosthetic. Thus the concentration and protein composition changes in diseased and periprosthetic SF.

The aim of the current paper was to study the 'inlet aggregation' mechanism in more detail and to quantify the effect of protein content and load (pressure) on film formation and CoCrMo wear.

2. Experimental programme

In the current work the MoM hip contact was simulated by a commercial grade 'as-cast' CoCrMo femoral head loaded and rubbing against a glass disc. Central film thickness was measured for a range of speeds, loads (pressures) and lubricant properties (BCS and proteins). Two series of tests were carried out:

1. Film formation under cyclic loading (5 N) at 0 mm/s (720 s). The contact was loaded for ca 15 s while film thickness measurements were taken and then un-loaded for ca 45 s, this was repeated every minute. Fresh fluid was continuously supplied to the contact.
2. Film formation and wear measurements at constant entrainment speed (10 mm/s) for 720 s (14.4 m sliding distance). Film thickness was measured during the test and periodically the wear scar diameter was estimated from the dispersed image. The following tests were then carried out after this initial constant speed test:
   a. Effect of load (5–20 N) on film thickness at 10 mm/s.
   b. Film thickness as a function of speed at constant load (5 N): tests were carried out by slowly increasing and decreasing the sliding speed (0–55 mm/s).

Film thickness was measured by thin film optical interferometry using a femoral head/glass disc contact. The test device was supplied by PCS Instruments PLC, London. The optical measurement technique has been extensively reported in earlier papers (Cann et al., 1996; Johnston et al., 1991) and only a brief description will be given here. The technique uses optical interferometry to measure central film thickness in the glass/metal contact region, the measurement

range is 1–1000 nm. A diagram of the test method is shown in Fig. 2(a). The underside of the glass disc is coated with a thin chromium layer (~10 nm) overlaid by silica (~500 nm); this provides the necessary reflection condition to measure the film thickness in the glass/metal interface. Incorporating the spacer layer method and spectrometric light dispersion, highly repeatable thin film measurements of 1–2 nm are possible (Myant, 2010; Spikes, 1999).

In earlier work (Fan et al., 2011) it was observed that a wear scar formed on the femoral head within a few minutes of the start of the test. It was possible to estimate the diameter of the contact and thus the wear scar from the optical interferometric image taken during the film thickness measurement. This is shown schematically in Fig. 2(b). For an initial static contact (5 N) the effective contact width was estimated to be 230 μm, which compared to a calculated Hertzian width of 220 μm. One of the problems of the earlier results was the time dependency of the film thickness. In the current study film formation was measured at a constant entrainment speed (10 mm/s) until the film had stabilised, load and variable speed tests were then conducted immediately afterwards.

It was possible to monitor wear of the CoCrMo head during the sliding tests from the optical interferometric image. It must be emphasised that these tests were not originally intended to produce wear of the CoCrMo surface; however it was observed that the apparent contact area increased during the test. Post-test examination revealed that a circular wear scar had formed on the femoral head (see Fig. 1); this was particularly surprising as the silica coating was, in most cases, undamaged. The wear also occurred very quickly and the contact width growth was apparent within a few minutes of the start of the test. The initial test configuration is a ball-on-flat and clearly wear of the CoCrMo surface produces a flat-on-flat contact which decreases the effective pressure as the load is supported by an increasing contact area. The changing contact pressure might be responsible for the increasing film thickness which develops as the test progresses; this has been reported in an earlier paper (Fan et al., 2011). The new tests were designed to allow the film thickness (and effective contact pressure) to stabilise, it was then possible to study the effect of load and speed on film formation.

It is also possible to observe film formation (Cann et al., 1996) by taking images directly from the rubbing contact. The film thickness distribution is seen as different coloured areas within the contact region. Some examples are given at the end of the paper; this approach will be reported in more detail in a later paper.

The test specimens were cleaned ultrasonically in 1% sodium dodecyl sulphonate solution in deionised water. The specimens were then rinsed three times in deionised water and finally washed in Analar isopropanol. Before the test specimens were air-dried and then mounted in the optical device, which was held at 37 °C for 1 h prior to testing. The test solution was fed directly into the contact zone using a syringe to prevent contamination. The solution was pre-warmed before entering the contact by flowing through silicone tubing held in a heated water bath at 35 °C. The silicone tubing then passed through the heated chamber of the test device. The flow rate was controlled to maintain a substantial fluid meniscus around the contact zone. The test conditions were chosen to be representative of those occurring during the gait cycle in MoM hip joints. The initial load was 5 N which corresponds to mean Hertzian pressures of 120 MPa. However this dropped to an estimated 60 MPa once the wear scar was formed. The cyclic load tests were carried out twice (these were very repeatable), the wear tests (constant entrainment speed, 10 mm/s) three times.

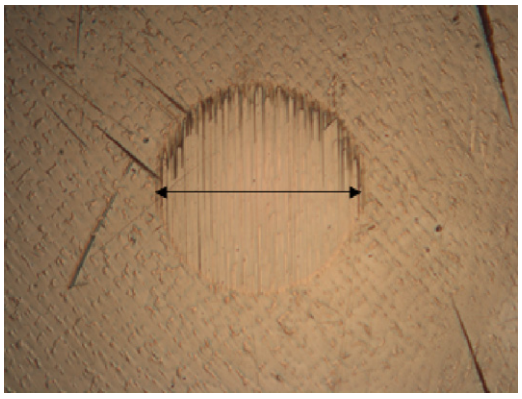

Fig. 1 – Low-power microscope image of wear scar on femoral head component. Contact width (indicated) 580 μm.

Table 1 – Experimental test conditions and fluids.

Test conditions:	
Temperature	37 °C
Test specimens	Glass disc—coated chromium and silica layers 38 mm diameter CoCrMo femoral head (as cast)
Constant speed tests:	
Mean speed	0, 10 mm/s 15 m sliding distance
Load	5 N (initial mean Hertz pressure: 113 MPa)
Variable load tests	
Load	5–20 N (estimated Hertz pressure: 60–80 MPa)
Mean speed	10 mm/s
Variable speed tests:	
Mean speed	0–55 mm/s
Load	5 N (estimated Hertz pressure: 60 MPa)
Test solutions:	
BCS25	Bovine calf serum 13 mg/ml total protein
Alb10	Albumin: 10 mg/ml saline solution
Alb20	Albumin: 20 mg/ml saline solution
Alb30	Albumin: 30 mg/ml saline solution
Glb6	γ-globulin: 6 mg/ml saline solution

Bovine calf serum (Sigma Aldrich 12133C protein concentration 72 mg/ml) was used as a model synovial fluid and was diluted by deionised water (Sigma-Aldrich, S-37531-356) to 25% w/w. Albumin (bovine serum albumin Sigma Aldrich A7906) and γ-globulin (bovine γ-globulin Sigma Aldrich 4030) were prepared as different concentrations in physiological saline solution (150 mM NaCl solution in deionised water). All fluids were stored at 5 °C and used within a few days of preparation. The experimental test conditions are summarised in Table 1.

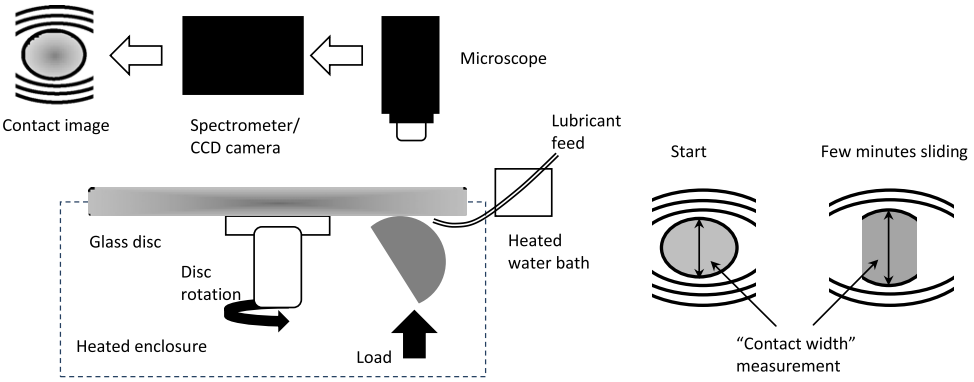

(a) Test device.

(b) Schematic of contact width measurement: image dispersed through a grating spectrometer.

Fig. 2 – Schematic diagrams of film thickness and contact width measurement methods.

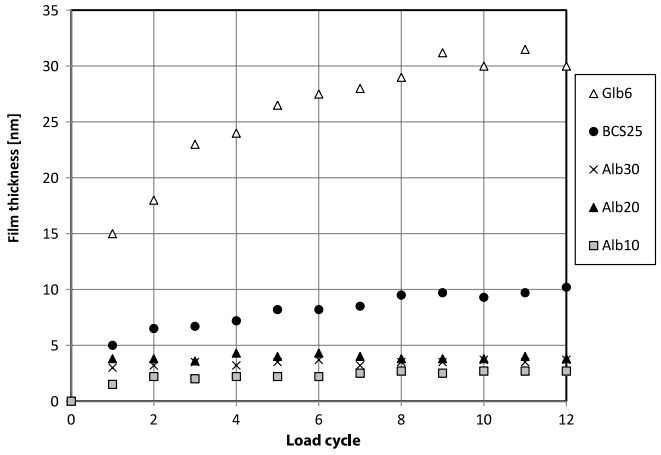

Fig. 3 – Film thickness results for cyclic loaded tests versus load cycle number for all solutions. Each load cycle represents 60 s.

3. Results

3.1. *Constant speed film thickness results*

Central film thickness results for all test solutions under cyclic loading conditions (zero entrainment speed) are plotted in Fig. 3 against load cycle number. Repeatability was very good and typical results are shown. Film increase with time was observed for all fluids; the order of film formation was:

Glb6 ≫ BCS25 > Alb30 > Alb20 > Alb10.

Constant speed (10 mm/s) film results are shown in Figs. 4 and 5. Typical results are shown in Fig. 4(a) for BCS25 and Fig. 4(b) for Alb20, the results from the cyclic load tests are also shown (all plotted against time). Constant speed tests (constant load) for all solutions are summarised in Fig. 5 where average film thickness is plotted against sliding distance. The film thickness ranking at the end of the test was:

Glb6(>100 nm) ≫ Alb30(ca 40 nm) > BCS25,
Alb20, Alb10(ca 35 nm).

3.2. *Effect of load on film thickness*

At the end of the constant speed tests the effect of increased load (contact pressure) on film thickness was investigated. The load was increased from 5 to 20 N whilst keeping the speed constant (10 mm/s). Typical results are plotted in Fig. 6(a) as film thickness as a function of load for Alb20 and Glb6 samples; similar results were recorded for all the test fluids. The film thickness decreased rapidly with increasing load; at 20 N it typically dropped to less than 50% of the original value measured at 5 N. The load dependencies used by Hooke (1980) ($h \sim W^{-0.13}$) and Dowson (2006) ($h \sim W^{-0.21}$) are also shown for a fluid with a nominal viscosity of 0.1 Pa s. The analysis also provides a rough estimate for the viscosity of the fluid entering the contact region as this is much greater than predicted from the high-shear rate values of these fluids. Curve-fitting of the experimental results gives a load power exponent of −0.5 to −1.3 depending on the fluid. Higher exponents were recorded for the Glb6 fluids as the contact pressures were much greater. The Glb6 tests did not form a

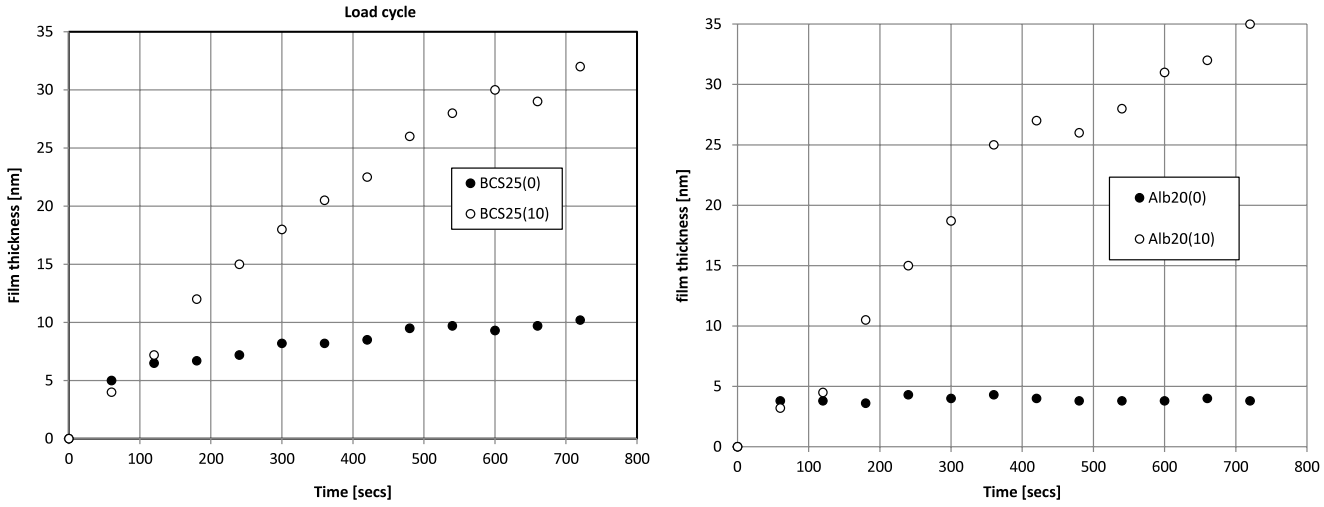

(a) BCS25 solutions. **(b) Alb20 solutions.**

Fig. 4 – Film thickness plotted against time for 0 (cyclic load) and 10 (constant load) mm/s tests for BCS25 and Alb20 fluids.

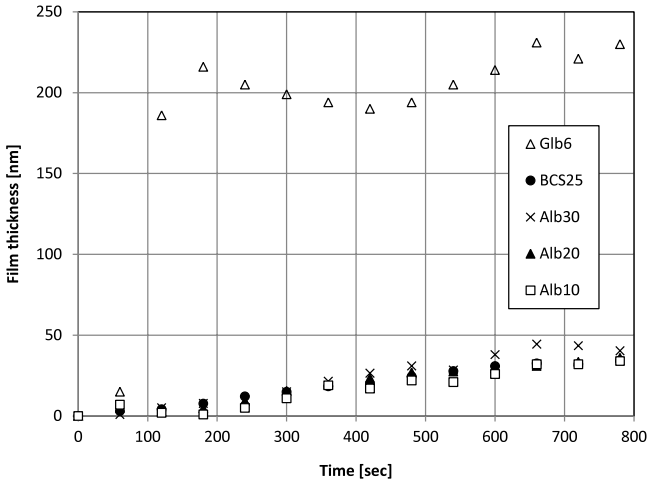

Fig. 5 – Central film thickness plotted against time for all test solutions under constant load and entrainment speed (10 mm/s).

significant wear scar and thus the contact pressure range for the same load was much larger in this case.

The contact films recovered rapidly once the load was decreased; this is shown in Fig. 6(b) where the effect of increasing (5–20 N) and decreasing load (20–5 N) is demonstrated for an Alb30 residual film in a static contact (0 mm/s). The film reduced with increased load and then recovered once the load was dropped to 5 N.

3.3. *Variable speed film thickness results*

At the end of the constant speed tests a variable speed (increasing/decreasing) test was carried out and film thickness was measured over the speed range at 5 N. Due to the formation of a wear scar the mean contact pressure was reduced from the initial levels and was estimated to be ~60 MPa. Central film thickness is plotted as a function of mean speed in Fig. 7 for albumin and BCS solutions. The corresponding results for globulin were very difficult to measure; as the film thickness varied within the contact zone and was typically >200 nm. These results are not shown.

The albumin and BCS results demonstrate two distinct types of speed dependence depending on the protein concentration. The lower albumin concentration fluids (Alb10, Alb20) gave an increasing film with speed which corresponds to EHL predictions. The higher albumin fluids (Alb30) and BCS25 gave the thickest films at the lowest speeds, which is the inverse of the EHL predictions.

At 40 mm/s the film thickness order was:

Alb10(ca 60 nm) > Alb20(ca 45 nm) > Alb30, BCS25(ca 35 nm).

At 5 mm/s the film thickness order was:

Alb30, BCS25(ca 50 nm) > Alb20, Alb10(35 nm).

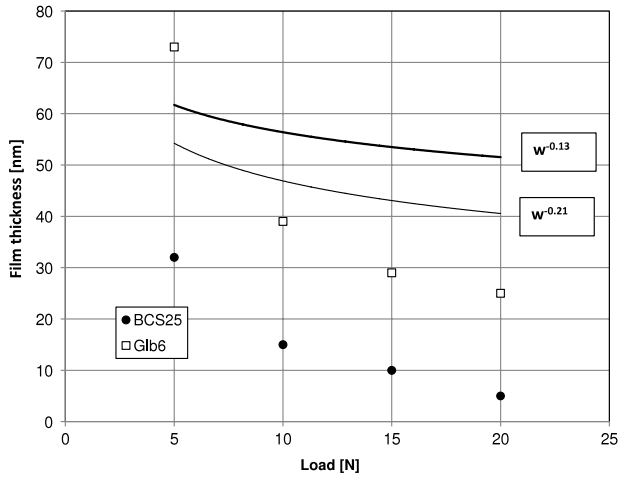

(a) Film thickness as a function of load for BCS25 and Glb6. Theoretical results ($\eta = 0.1$ Pa s).

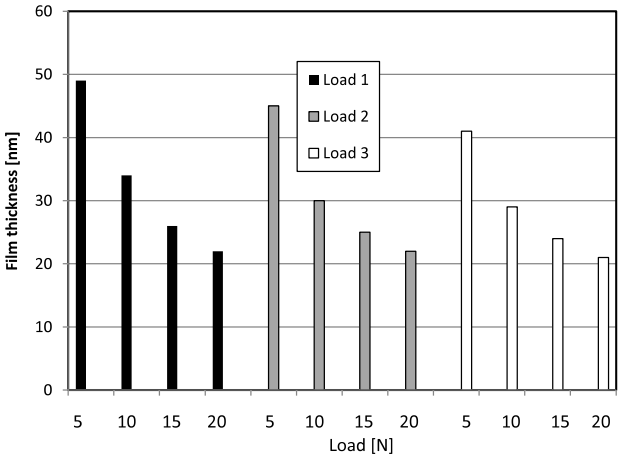

(b) Effect of repeated increasing and decreasing load on Alb30 film thickness (0 mm/s).

Fig. 6 – Effect of load on film thickness films formed at 10 mm/s.

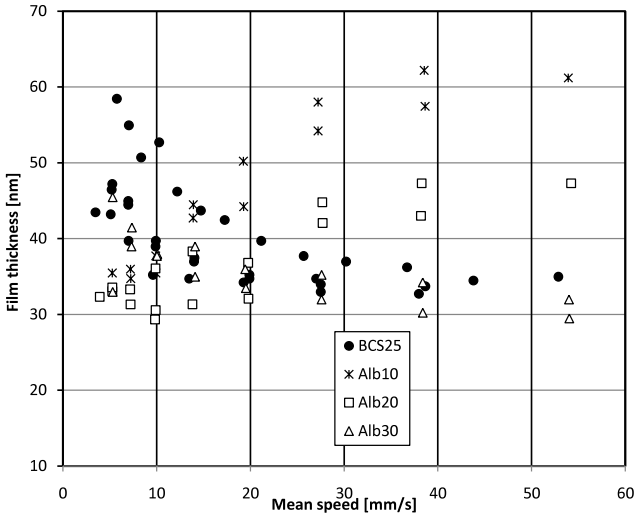

Fig. 7 – Film thickness plotted against mean speed at the end of the wear tests for albumin and BCS solutions.

3.4. *Wear scar measurement*

The effective contact width was measured during the constant speed tests and example results are shown in Fig. 8, where "effective contact width" is plotted as a function of (disc) sliding distance. The initial width measurements were 98–102 pixels, which corresponds to 225–235 μm. The calculated Hertzian contact width for 5 N, CoCrMo against glass is 220 μm. The final 'contact width' results are summarised in Fig. 9. These are plotted as relative contact width change (CW_r) where $CW_r = CW_{end}/CW_{start}$. CW_{start} and CW_{end} were measured at zero speed and 5 N load. Effective wear scar width at the end of the 10 mm/s contact speed test was:

Alb20, Alb10 > ALB30, BCS25 ≫ Glb6.

At the end of the test the femoral head was removed, rinsed with deionised water and the wear scar examined under a low-power microscope. Images for Alb20 (X5 objective) and Glb6 (X10 objective) are shown in Fig. 10. The wear scar for the albumin test is clearly observed; this is approximately 400 μm in diameter. The wear scar for the globulin tests is much smaller and not clearly defined; the surface appears to be polished rather than having suffered significant material loss. We are currently carrying out surface roughness measurements of the wear scar to characterise these changes. The globulin contact area is covered in gel-like deposits particularly in the inlet region, these deposits were very difficult to remove and survived repeated rinsing.

4. Discussion

The results have demonstrated the very different film formation and wear properties of the protein containing solutions. Under cyclic loading conditions a gradual increase in film thickness was observed for all protein containing solutions. This time dependent deposition of proteins has been observed previously (Malmsten, 1998). It is well known that most proteins preferentially absorb onto hydrophobic rather than hydrophilic surfaces (Malmsten, 1998), therefore, it is likely that the observed protein layer is predominately on the CoCrMo surface. Indeed, post test microscope analyses revealed that proteins absorbed onto the femoral head well outside of the contact area (ultra low flow/shear conditions) or when the femoral head was left to soak in solution (no load or flow/shear). However, this absorbed layer was weak and easily removed with light rinsing of the femoral surface with water. The cyclic loading may aid, or accelerate, this deposition process to form robust protein films by increasing protein–protein interaction, transportation of proteins to the surface and rearranging or reorientating the absorbed

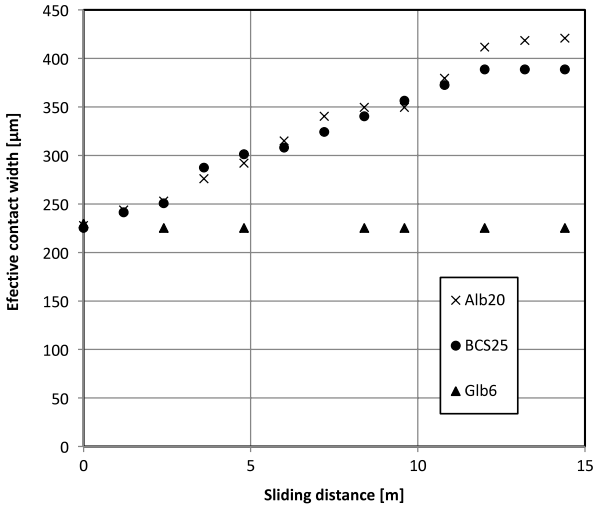

Fig. 8 – Example of effective contact width measurements (plotted against sliding distance) for Alb20, Glb6 and BCS25 taken during the constant speed tests.

protein structure. The effects of protein-surface interactions has large implications for the selection of bearing material pairing; *i.e.* the change in surface hydrophobicity with ceramic-on-ceramic, or more likely metal-on-polymer artificial joints. The authors hope to extend the current research to cover these material pairs, however, some experimental development is required.

In the constant speed tests film thickness increased with sliding distance (time) for the albumin and BCS solutions. However, rapid wear of the CoCrMo surface occurred, significantly increasing contact size and thereby reducing the contact pressure. The gradually increasing films for albumin and BCS containing fluids could be attributed to decreasing contact pressure rather than deposition of surface films.

The films for the globulin solutions were very difficult to measure as they were very thick; in some cases >200 nm. Multiple interference orders were observed in the contact region and it was impossible to assign a single film thickness value. It would be expected that such thick globulin films effectively protect the femoral head from wear. Post-test examination of the rubbed area showed this was defined by the formation of a thick gelatinous deposit mainly in

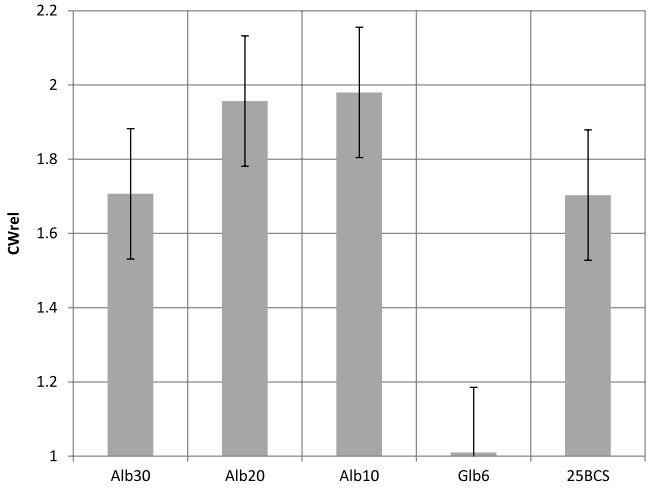

Fig. 9 – Summary of effective CW_r measurements for test fluids. %error bars plotted.

(a) Alb20 wear scar (x5 objective). **(b) Glb6 wear scar (x10 objective).**

Fig. 10 – Low power microscope images from the femoral head wear scar at the end of the test after light rinsing with water.

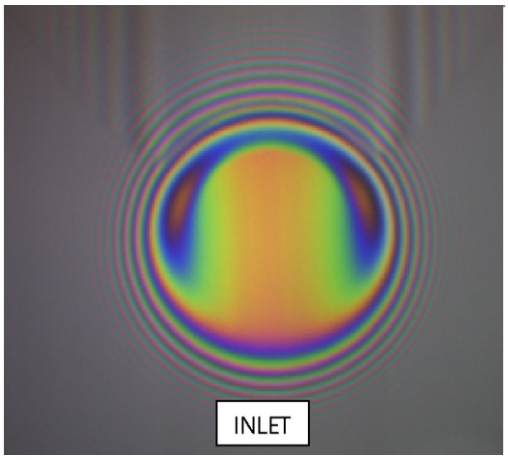

(a) Optical interferometric image from a rolling contact lubricated by hydrocarbon oil.

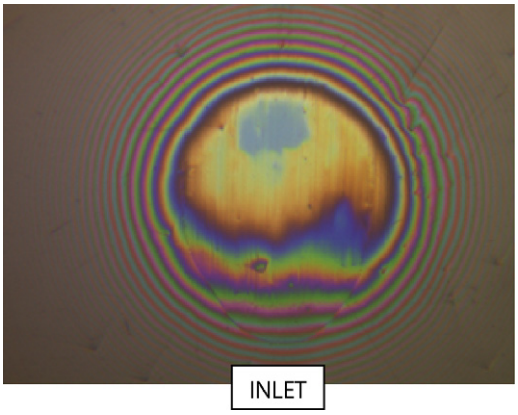

(b) Optical interferometric image from a low-speed sliding contact lubricated by bovine serum.

Fig. 11 – Optical interferometric images of lubricant films.

the inlet region. Light polishing of the Hertzian region and removal of the carbides was also observed. For the contact of interest (CoCrMo/Glass) proteins were observed to adhere strongly to the CoCrMo surface only. In a CoCrMo/CoCrMo contact it would not be unreasonable to assume proteins may therefore adhere to both contacting surfaces. This may affect the overall wear rate, or time dependent film thickness behaviour, but is unlikely to significantly alter the lubrication process.

The observation of surface damage to the CoCrMo head during these tests was surprising. The rubbing counterface is a thin silica layer 500 nm thick deposited on a chromium semi-reflective layer. In other work with hydrocarbon fluids and steel surfaces we have found the silica layer to be rapidly destroyed once sliding is imposed. In this study the silica layer was largely undamaged although some scratches were observed. The CoCrMo surface however was rapidly worn. Post test microscopy analysis of femoral surface revealed two possible wear mechanisms:

1. 3rd body abrasion due to the loss of femoral surface block carbides associated with the as-cast alloy (Fan et al., 2011). This wear debris is likely to be entrained into the contact or embed in the glass disc and cause the scratches seen on the CoCrMo surface (see Fig. 1). Surface topography measurements showing loss of carbides in the wear scar were shown in earlier work (Fan et al., 2011).
2. "Chemical polishing" of the contact area possibly due to tribo-corrosion mechanisms associated with the proteins adsorbed at the surface (Lewis et al., 2006). Globulin is reported to promote chromium dissolution less than albumin (Lewis et al., 2006).

The wear results showed very clearly the effect of protein type and to a lesser extent the effect of protein concentration. The globulin containing fluids gave significantly lower wear than the albumin or BCS solutions. Wear appeared to reduce with increasing protein content although this effect was less marked. These results suggest that different protein concentrations and composition (Kitano et al., 2001) occurring in periprosthetic SF would significantly influence implant wear. It is possible that globulin has a dual role; physical protection of the surfaces by the formation of a thick interfacial film and blocking metal ion removal from the surface layers.

In an earlier paper (Fan et al., 2011) the authors introduced the idea of a protein aggregation lubrication mechanism. Shear aggregation of protein molecules forms a reservoir of highly viscous material in the inlet which passes through the contact forming a separating film in the contact region. The work presented in this paper supports this hypothesis and provides further insight into the contribution of different proteins to the mechanism. The globulin solutions formed very thick films which survived post-test cleaning as gelatinous deposits in and around the contact region. The in-contact optical interference images for the protein fluids show very different films to those obtained with simple hydrocarbon oils (Fig. 11). Fig. 1(a) shows a classical EHL film formation with the constant thickness central region and film constrictions at the rear and side. The protein image in Fig. 11(b) is very different. The film thickness decreases markedly within the contact zone under the increasing pressure field due to layer compression.

Gel formation in the inlet region was particularly marked for the globulin containing solutions as seen in Fig. 1(b). It is likely that the ability of the proteins to form aggregates within the contact inlet determines the lubricant performance. For this globulin is well suited; it has a greater molecular weight (~140 K Da compared to ~60 K Da for albumin) and is less soluble and therefore more likely to fall out of solution (separate from the bulk phase) compared to albumin. There is substantial support for the 'inlet-aggregation' mechanism in the research literature. Synovial fluid and albumin containing fluids are known to be rheopectic at low shear rates (Oates et al., 2006). Oates et al. (2006) attributed this rheopectic behaviour to association of protein molecules under shear to form gel networks. The formation of protein precipitates

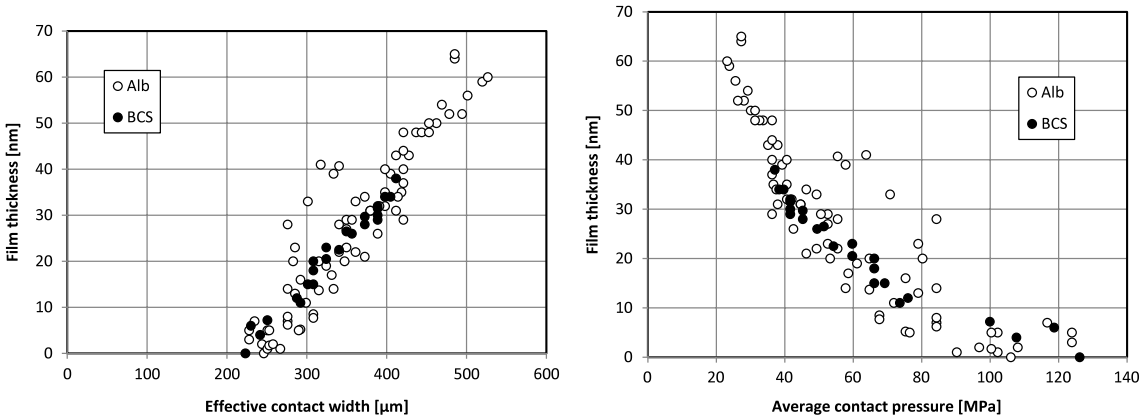

(a) Film thickness vs. effective contact width measured during 10 mm/s tests.

(b) Film thickness vs. estimated average contact pressure from the above graph.

Fig. 12 – Film thickness plotted as a function of (a) effective contact width and (b) average contact pressure.

in lubricating fluid in simulator tests has been extensively reported (Lu and Mckellop, 1997). This is usually thought to be due to thermal precipitation of denatured proteins. In a recent paper Maskiewicz et al. (2010) analysed protein degradation products formed during simulator tests of serum-based lubricants. They reported the formation of "high molecular weight aggregates" which precipitated out of solution. There was no evidence of protein molecular fragmentation. The major conclusion from this work was that degradation was not due to frictional heating but that high shear rates within the articulating interface were responsible for protein agglomeration.

Once this gelatinous material is formed it behaves quite differently from the bulk solution. The variable speed film thickness results were surprising (Fig. 7); at low albumin concentrations film thickness increases with entrainment speed. However, for thick film forming solutions, or gel like films (globulin and high albumin concentrations), an inverse dependency is seen. On approaching the contact inlet material in the suspension is subjected to off axis fluid forces as the majority of lubricant flows around the contact, not through it. Only material on the central streamline will pass through the contact (Dwyer-Joyce, 1993). It is likely that as larger aggregates are formed within the inlet reservoir they become subjected to larger off axis fluid forces, which will increase with speed.

The reason for the film thickness 'inversion' at high speeds where "low concentration" is greater than the "high concentration" is not understood and is the subject of further study. However the results do emphasise the importance of not treating these protein-containing solutions as simple continuum fluids with a single representative viscosity. In an earlier study (Fan et al., 2011) the high-shear rate viscosity was measured for a range of BCS fluids (25%–100%) and very similar results (~0.021–0.026 Pa s) were obtained. The differences only become apparent in the fluid behaviour close to the contact.

Gel film thickness was found to be very sensitive to load (contact pressure) which is shown in Fig. 6. Additional analysis of the results is shown in Fig. 12(a) where film thickness is plotted against effective contact width for all albumin/BCS25 tests at 10 mm/s. Film thickness increases with increasing contact width (wear) and thus decreasing effective contact pressure. It is possible to estimate an average contact pressure from these results (load/effective contact area) and the film results are replotted against this estimated contact pressure in Fig. 12(b). It is interesting to compare the contact pressure range to that experienced by MoM hip joints during articulation. A simple Hertz analysis for a maximum load of 3500 N gives mean contact pressures that range from ~ 120 MPa for a 28 mm diameter head with 100 μm radial clearance to ~30 MPa for a 56 mm diameter head with 50 μm radial clearance. The gel-film thickness is very sensitive to pressure in this range and this observation might explain the better wear performance obtained for LHMoM joints in simulator tests (Smith et al., 2011).

These results suggest that protein containing lubricating films are exceptionally sensitive to increased contact pressure and are thus more likely to fail in edge loaded hips. The gel film within the contact is formed by a complex matrix of proteins and it is possible this matrix has 'sponge' like properties. Under low pressure the matrix is filled by the aqueous suspension medium, as the pressure (load) increases this fluid is squeezed out and ejected from the contact. This would account for the significant reduction in film thickness with increasing load (Fig. 6(b)). Recovery of the gel film thickness was observed after the removal of load; capillary action sucks fluid back into the matrix 're-inflating' the gel/sponge. The recovery of the film thickness under repeated loading would suggest it has elastic properties.

The lubrication mechanism proposed in this paper is very different to classical EHL models as these are usually based on an isoviscous, incompressible physical model. The results from this study suggest that the bulk fluid properties are conditioned by flow in and around the contact zone giving a reservoir of high-viscosity material in the inlet region. The separating films are formed by thin adsorbed film augmented by a "gel" layer. The gel is deposited on static surfaces forming

the "protein deposits" observed on implants from simulator and explant studies (Wang et al., 1998; Wimmer et al., 2003). Some of the observations from these earlier studies support our findings for example Wang et al. (1998) concluded that 'soluble' proteins did not contribute to the lubrication process and that wear protection came from the insoluble deposits.

The results from our study, if applied to artificial hip joints, have obvious implications for component design and implantation. The increased head diameter of the resurfacing and LHMoM hips results in higher sliding speeds during articulation. Our study suggests this leads to a decreasing film thickness for high protein-contents which typically are present in periprosthetic SF. However the decrease in contact pressure due to increased head size and reduced clearance will tend to increase film thickness. Edge-loading due to cup misalignment may result in local increases in contact pressure and thus significant decrease in the 'gel' lubricating film.

It should be noted that the contact in this paper has undergone either cyclic loading with static entrainment (0 mm/s) or simple uni-directional sliding with constant load. A real hip undergoes bi-directional sliding with multiple flow axes and transient loading conditions. The reversal in flow direction and change in axis may slow, or prevent, the build up of a protective protein surface layer by removal of the inlet aggregates. This is currently under investigation.

5. Conclusions

The paper reports a fundamental investigation of protein film formation mechanisms in artificial hip joints. We conclude the following:

1. Protein-containing fluids form thin solid films (~4 nm) on the contact surfaces under repeated loading. γ-globulin-containing fluids formed significantly thicker films (~30 nm).
2. Globulin-containing lubricants significantly reduced CoCrMo wear compared to albumin-containing fluids. Effective wear scar width at the end of the 10 mm/s constant speed test was:

   Glb6 $\ll$ BCS25 $\sim$ Alb30, Alb20, Alb10.

3. The chemistry (protein content and type) of periprosthetic SF plays a role in determining implant wear.
4. A new lubricating mechanism is proposed for protein-containing fluids in sliding contacts. Film formation is controlled by the development of a high-viscosity reservoir in the inlet region; periodically this material passes through the contact locally increasing the film thickness.
5. The formation of the "gel reservoir" is due to shear-aggregation of protein (particularly globulin) molecules in the inlet flow field. The reservoir formation occurs predominately at low speeds and contributes significantly thicker films.
6. The protein gel lubricant films are very sensitive to contact pressure, they appear to be elastic and compressible (on average $h \sim W^{-0.7}$).
7. Film formation does not obey isoviscous, incompressible fluid predictions.

Acknowledgment

The authors wish to thank the UK EPSRC (Grant number EP/H020837/1 "In-contact Analysis of Synovial Fluid Lubricating Film Properties") for supporting this research.

REFERENCES

Bell, J., et al., 2001. The influence of phospholipid concentration in protein-containing lubricants on the wear of ultra-high molecular weight polyethylene in artificial hip joints. Proc. Inst. Mech. Eng. H 215, 259–263.

Cann, P.M., et al., 1996. The development of a spacer layer imaging method (SLIM). Tribol. Trans. 39, 915–921.

Cooke, A.F., et al., 1978. The rheology of synovial fluid and some potential synthetic lubricants for degenerate synovial joints. Proc. Inst. Mech. Eng. H. 7, 66–72.

Delecrin, J., et al., 1994. Changes in joint fluid after total arthoplasty. Clin. Orthop. Relat. Res. 307, 240–249.

Dowson, D., 2006. Tribological principles in metal-on-metal hip joint design. Proc. Inst. Mech. Eng. H 220, 161–171.

Dwyer-Joyce, R.S., 1993. The effects of lubricant contamination in rolling element performance. Ph.D. Thesis. Imperial College: University of London Press.

Fan, J., et al., 2011. Inlet protein aggregation: a new mechanism for lubricating film formation with model synovial fluids. Proc. Inst. Mech. Eng. H 225, 696–709.

Hooke, C.J., 1980. The elastohydrodynamic lubrication of heavily-loaded point contacts. J. Mech. Eng. Sci. 22, 183–187.

Johnston, G.J., et al., 1991. The measurement and study of very thin lubricant films in concentrated contacts. Tribol. Trans. 34, 187–194.

Kitano, T., et al., 2001. Constituents and pH changes in protein rich hyaluronan solution affect the biotribological properties of artificial articular joints. J. Biomech. 34, 1031–1037.

Langton, D., et al., 2008. The effect of component size and orientation on the concentrations of metal ions after resurfacing arthroplasty of the hip. J. Bone Joint Surg. Br. 90 (9), 1143–1150.

Lewis, A.C., et al., 2006. The entrapment of corrosion products from CoCr implant alloys in the deposits of calcium phosphate: a comparison of serum, synovial fluid, albumin, EDTA, and water. J. Orthop. Res. 1587–1596.

Lu, Z., Mckellop, H., 1997. Frictional heating of bearing materials tested in a lubricant in a hip joint wear simulator. Proc. Inst. Mech. Eng. H 211, 101–107.

Malmsten, M., 1998. Formation of absorbed protein layers. J. Colloid Interface Sci. 207, 186–199.

Maskiewicz, V.K., et al., 2010. Characterization of protein degradation in serum-based lubricants during simulation wear testing of metal-on-metal hip prostheses. J. Biomed. Mater. Res. Part B 94, 429–440.

MHRA, 2010. Medical Device Alert, April.

Myant, C., 2010. Experimental techniques for investigating lubricated, compliant, contacts. Thesis. Imperial College Press.

National Joint Registry, 2010. 7th Annual Report.

Oates, K., et al., 2006. Rheopexy of synovial fluid and protein aggregation. J. R. Soc. Interface 3, 167–174.

Revell, P.A., et al., 1997. Biological reaction to debris in relation to joint prostheses. Proc. Inst. Mech. Eng. H 211, 187–197.

Sawae, Y., et al., 2008. Influence of protein and lipid concentration of the test lubricant on the wear of ultra-high molecular weight polyethylene. Tribol. Int. 41, 648–656.

Smith, S.I., et al., 2011. The effect of femoral head diameter upon lubrication and wear of metal-on-metal total hip replacements. Proc. Inst. Mech. Eng. H 215, 161–170.

Spikes, H., 1999. Thin films in elastohydrodynamic lubrication: the contribution of experiment. Proc. Inst. Mech. Eng. J 213, 335–352.

Wang, A., et al., 1998. Lubrication and wear of ultra-high molecular weight polyethylene in total joint replacements. Tribol. Int. 31, 17–33.

Wang, A., et al., 2003. The effects of lubricant composition on in vitro wear testing of polymeric acetabular components. J. Biomed. Mater. Res. Part B 68B, 45–52.

Widmer, M.R., et al., 2001. Influence of polymer surface chemistry on frictional properties under protein-lubrication conditions: implications for hip-implant design. Tribol. Lett. 10, 111–116.

Wimmer, M.A., et al., 2003. Tribochemical reaction on metal-on-metal hip joint bearings. A comparison between in-vitro and in-vivo results. Wear 255, 1007–1014.